Designing and Building a 3D-Printed Quad-Tiltrotor UAV Using ArduPilot

Akshaj Goel
Student
United World College of South East Asia
Singapore
akshaj.goel@gmail.com

***Abstract* —** This technical report outlines the design and building process of a Quad-Tiltrotor Unmanned Aerial Vehicle (UAV), a type of drone. While this technology has been thoroughly explored for fixed-wing planes, its application to quad-setups is less common and has room for innovation. The quad-tiltrotor UAV is built around a 3D-printed frame and uses open-source ArduPilot firmware through a Matek H743-WLite flight controller, running on a 6S power system. It consists of four servo-driven arms independent of the main body that are capable of rotation. This enables thrust vectoring by the motors while the drone's body remains flat and stable during forward motion. Keeping the body level reduces frontal area in forward flight, which is expected to lower aerodynamic drag and therefore energy consumption per flight**.** Based on flight-log data, the main body's pitch stayed within approximately 6.5° of level during forward flight. This report consists of six distinct stages: *Concept*, *Rotation Mechanism*, *Components & Circuitry*, *Chassis Design*, *Fabrication & Assembly*, and *Control Setup*.

Aim and Objectives

The aim of this project was to design, build, and test a fully functional quad-tiltrotor UAV that achieves stable, aerodynamically efficient forward flight by independently rotating its arms, rather than relying on differential motor speeds as in a conventional quadcopter.

To achieve this aim, the project was broken down into the following objectives:

1. Design a rotation mechanism capable of tilting each drone arm independently and reliably under the load of a motor.
2. Use a set of compatible electronic components (flight controller, ESCs, motors, battery, radio system) capable of supporting both propulsion and tilt functions.
3. Design and 3D-print a chassis that accommodates the rotation mechanism, electronics, and battery, all while remaining fairly lightweight.
4. Fabricate and assemble the physical drone from all designed and printed components.
5. Configure ArduPilot's firmware to enable tilt-based flight control, and test the drone to confirm stable hover and transition flight.

To judge whether the aim had been achieved, each objective was given a measurable success criterion, defined before testing began:

1. **Rotation mechanism:** each arm rotates through its full tilt range and holds its angle under motor load, with no slipping, cracking or visible wobble. This was checked with a bench test at hover throttle, observed visually and on video.
2. **Electronics:** all four motors, ESCs and servos respond correctly to radio input, with no power loss or overheating. This was checked with motor and servo tests in Mission Planner, battery voltage and current readings, and a temperature check of the ESCs and PDB after flights.
3. **Chassis:** the chassis holds every component securely and the finished drone can lift off and hover. This was checked by visual inspection after each flight and by the hover throttle in the flight log.
4. **Fabrication and assembly:** the built drone matches the CAD design and no printed part fails during testing. This was checked by inspecting all printed parts after each flight.
5. **Control and flight:** the drone hovers stably and flies forward under control, with the main body staying close to level while the arms tilt. This was checked using the pitch angle recorded in the Mission Planner flight log during forward flight.

The overall aim would be considered achieved if all five criteria were met. Criterion 5 matters most, since it directly tests whether rotating the arms keeps the body flat.

I. CONCEPT

All drones utilise the concept of thrust-vectoring for forward motion. As shown in *Figure 1*, the thrust force from the motor has both horizontal and vertical components, helping with forward motion while also allowing it to hover midair.

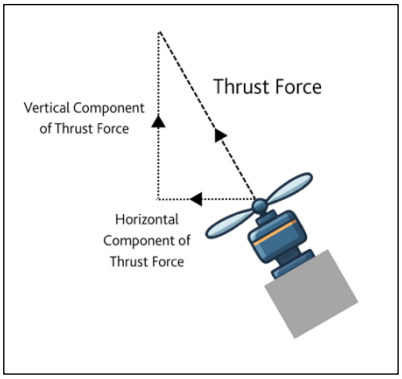


Figure 1: Diagram Depicting Thrust Vectoring by a Drone Motor

A traditional quadcopter drone with fixed arms will create the angled tilt by varying motor speeds in order to tilt the whole body. On the other hand, this project's quad-tiltrotor drone will instead create the angled tilt by independently rotating the arms, leading to the main body remaining flat and stable. Aside from stability, another advantage of this design is potential reduced aerodynamic drag due to a reduced frontal area. *Figure 2* and *Figure 3* compare the side aerodynamic profiles of a traditional quadcopter drone and this project's quad-tiltrotor drone during forward motion, showing airflow differences.

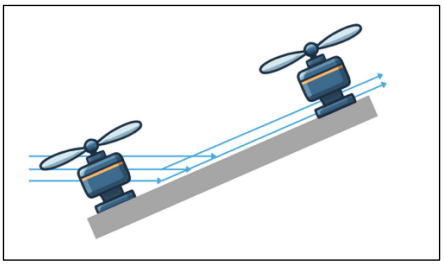


Figure 2: Side Profile of a Standard Quadcopter During Forward Motion; Blue Arrows Represent Airflow

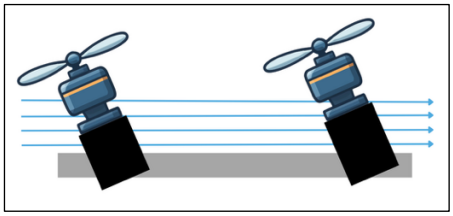


Figure 3: Side Profile of This Project's Quad-Tiltrotor Drone During Forward Motion; Blue Arrows Represent Airflow

Concept and Wider Purpose

If the concept works, the direct implications are a more stable sensor platform and potentially lower aerodynamic drag in forward flight, which could extend flight time per battery charge. The indirect implications are broader. A drone that needs less stabilisation hardware could be lighter and cheaper, which matters for low-cost application. Lower energy use per flight could modestly reduce the environmental footprint of drone operations. While servo motors could take up some energy, there will no longer be any need for front-back motor speed differentials, which can help reduce power draw. There are also trade-offs. The tilting mechanism adds moving parts that can wear or fail.

II. ROTATION MECHANISM

To begin, an initial concept 3D sketch was designed using Fusion360 computer aided design (CAD). *Figure 4* shows this, though it lacks internal detail

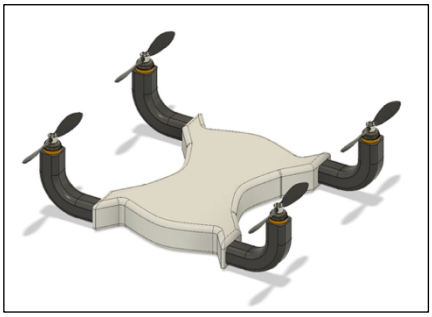


Figure 4: Initial Concept Sketch Without Internal Detail

The next step was to rework the design to include the detail of the rotation mechanism and make it hollow enough to give space for the circuitry. Moreover, a fully solid body would be significantly heavier and expensive. In the first detailed CAD design, the idea was to attach the servo motor directly to the arm, as shown in *Figure 5* and *Figure 6*.

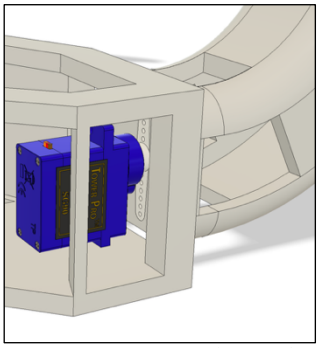


Figure 5: Servo Motor Directly Attached to Arm

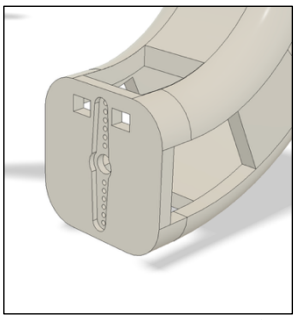


Figure 6: Engraving Into Arm to Directly Fit Servo Horn

The initial arm design in *Figure 6* shows how an engraving was made for the servo horn to tightly fit into, which could then be secured with M1 screws. The rectangular cut-outs were for the wires. A tight hole was also created under the servo motor to hold it in place. This initial concept was 3D-printed and tested out as shown in *Figure 7*.



Figure 7: Physical Printed Model of the First Rotation Mechanism Idea

A significant issue with this design was that the arm was leaning outwards, and that too even without the weight of a full drone motor. Along with that, rotation was very unstable, and the arm would keep shaking. The cause of this was that the servo motor was not designed to handle torque loads outside of its rotation plane, and this would worsen as the load increased.

To combat this, a new system was designed that ensured the servo motor only faced rotary loads and was in a more stable position. This included a servo stand, a rotary shaft piece, gears, and ball-bearings.

The first step was to stabilise the servo motor by placing it in a position where it would shake less, which was accomplished by creating a servo stand, as shown in *Figure 8*.

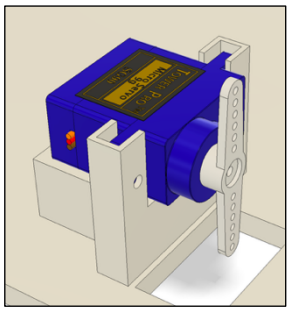


Figure 8: Servo Motor on Servo Stand

M2-sized holes were engraved for a screw to slot though the servo motor and the stand on both sides, holding it in place. Along with this, the servo motor was given a stable base to rest on, maximising stability.

The next step was to create the rotary shaft piece which had two functions: latch onto the servo horn to absorb rotary motion and transfer that motion to a gear. The piece that was designed is shown in *Figure 9*.

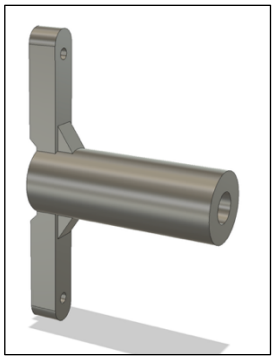


Figure 9: Rotary Shaft Piece

M1.2-sized holes were engraved at the top and bottom so that a screw could attach the rotary shaft piece to the servo horn. A slight space was given in the middle so that the servo screw could keep the horn attached to the servo motor. Triangular ribs were also added for rigidity. The hole at the end of the shaft was to guide an M3 threaded heat insert which would help with connecting the shaft to a gear.

The shaft piece was guided through a hole in the drone chassis, and a slot was added for a 609-series sealed ball-bearing. The bearing was to help stabilise the shaft and ensure it only had rotary motion without shaking at all. Afterwards, a spur gear was screwed into the end of the shaft piece. This system is shown in *Figure 10*, *Figure 11*, *Figure 12*.

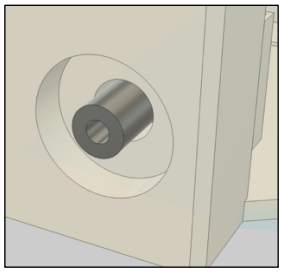


Figure 10: Rotary Shaft Piece Going Through a Hole Engraved in the Chassis

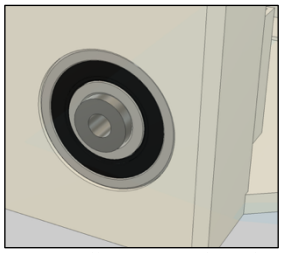


Figure 11: 609-series Ball-Bearing Slotted Into the Chassis to Stabilise the Rotary Shaft Piece

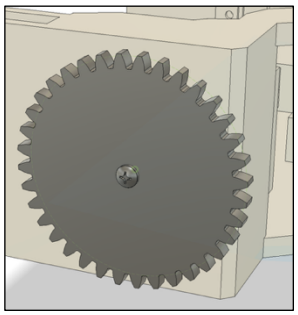


Figure 12: Spur Gear Screwed onto the Shaft with the Help of an M3 Threaded Heat Insert

The next step was to use the gear to drive the rotation of the drone arm. A 635-series ball-bearing was used to fit the arm in such a way that the gear would drive only its rotation, but other external forces would be transferred directly to the drone chassis which would be able to handle them better.

To do this, an arm piece with an in-built gear was designed, which had a hole to friction-fit the bearing. This was then fitted onto a small circular beam. This system is shown in *Figure 13*, *Figure 14*, and *Figure 15*.

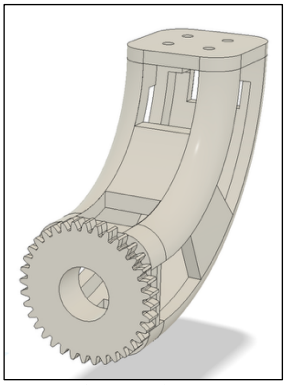


Figure 13: Arm Design With In-Built Spur Gear and Hole Engraved for Ball-Bearing

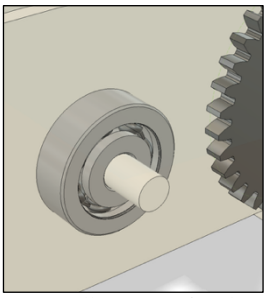


Figure 14: 635-series Ball-Bearing fitted onto Circular Beam

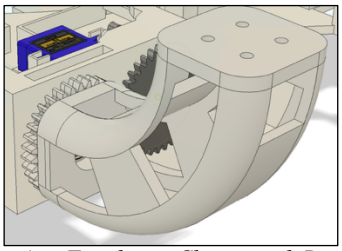


Figure 15: Drone Arm Fitted onto Chassis with Bearing and Meshed with the Rotation Gear

This new and improved rotation system seemed far more stable and was 3D-printed for testing, as shown in *Figure 16*.

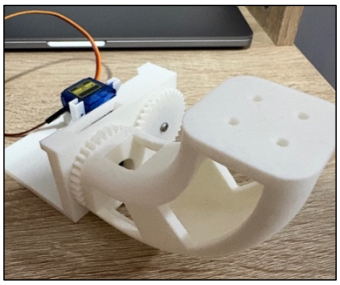


Figure 16: 3D-Printed Rotation Mechanism

Choosing a gear-driven rotary shaft supported by dual ball bearings over a direct-servo mount solved the outward bending moment problem. However, this choice introduced minor mechanical backlash between the gear teeth, which contributed to slight motor arm oscillation during tilt transitions, though it was pretty insignificant. Regardless, this was successful and far more stable.

All fittings were accurate and worked well, thus the rotation mechanism was complete. After testing, the initial gear was also superglued to the shaft to add an extra securing method on top of the screw, as it occasionally got slightly loose.

To design the rest of the chassis, measurements from the drone circuitry needed to be known, thus this was left for a later stage.

III. COMPONENTS & CIRCUITRY

To begin, a generic list of key drone components was compiled (excluding bearings/gears from earlier as those were already finalised), after which each component was carefully selected.

Component	Qty.	Purpose
Flight Controller (FC)	1	Control Core Functions
Electronic Speed Controllers (ESCs)	4	Direct Power to Propulsion Motors
Propulsion Motors	4	Spin Propellers at Rapid Speeds
Drone Propellers	4	Create Lift to Allow Flight
Servo Motors	4	Tilt Drone Arms
Power Distribution Board (PDB)	1	Allocate Battery Power to ESCs and FC
Drone Battery	1	Provide Battery Power to PDB
Radio Controller (RC)	1	Allow Remote Control of Drone
Radio Receiver	1	Receive Signals from RC and send them to FC
M10+GPS	1	

Table 1: Overview Table of Key Circuitry Components

The chosen flight controller board was a Matek H743-WLite, shown in *Figure 17*. This was primarily chosen due to its native support for ArduPilot firmware which enables tilt functions. It was cost effective, giving 13 PWM outputs, an onboard servo BEC, an in-built ICM42688-P IMU, a DPS310 barometer, 7 UART buses, 2 I^2C buses, 1 CAN bus, and an AT7456E OSD chip, all for a reasonable price. The dimensions of the double-layered board are 44 x 29 x 14.5 mm, with a weight of ~22g including the USB-C adapter [3].

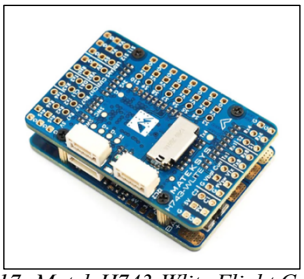


Figure 17: Matek H743-Wlite Flight Controller

The one catch with this flight controller was that it only provided 1 ESC pad pair, which was intended to be shared by 2 ESCs for a fixed-wing plane configuration. While fitting 4 ESCs was technically possible, it risked excess current concentration which could lead to dangerous heating. To bypass this, a power

distribution board was used, which would allow the ESCs to be powered by the battery without going through the flight controller.

The chosen propulsion motors were EMAX ECO II 2807 1300KV brushless motors, shown in *Figure 18*. This was due to their balance of thrust and efficiency. The 2807 stator paired with a relatively low 1300KV winding is optimised for 6–7 inch propellers, favouring high-torque thrust generation over high RPM output. It's also relatively cost effective, and is compatible with 3S-6S batteries [5].



Figure 18: EMAX ECO II 2807 1300KV Brushless Motor

The chosen ESCs were EMAX BLHeli 50 A ESCs, shown in *Figure 19*. With the chosen motors drawing a realistic peak of roughly 40–50A on 6S, and a rated maximum of ~52–59A under full throttle, a 50A ESC was selected for each of the four motors. This exceeds EMAX's own recommended 45A rating for this motor, providing margin over normal operating currents while remaining compact and lightweight. These ESCs are also from the same brand as the motors, ensuring compatibility, while also being cost effective [6].



Figure 19: EMAX BLHeli 50A ESC

The chosen power distribution board was a Matek PDB Hex 12S, shown in *Figure 20*. The Matek PDB Hex 12S offers six independent ESC power pads, each rated at 60A continuous. This is above the maximum possible current, drastically reducing the chance of failure. Its 140A continuous rating exceeds the maximum current the battery can deliver, ensuring the board is never the limiting element, while its integrated 264A current sensor feeds real-time battery monitoring to the flight controller and its overcurrent and short-circuit protection add electrical safety. The board's 2–12S input range accommodates a 6S battery [4].

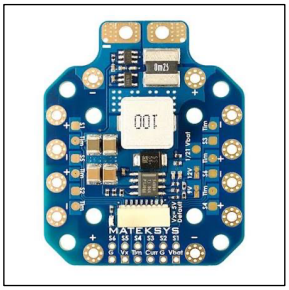


Figure 20: Matek PDB Hex 12S

The battery chosen was a 6S, 45C, 2800mAh, LiPo battery, as shown in *Figure 21*. 6S was chosen to match the low-KV motors, as a higher voltage allows the same power output to be delivered at lower current, reducing the load on the ESCs, PDB, and wiring. The selected 2800mAh 45C pack supplies 126A of continuous current, which covers the aircraft's hovering and transition demands while providing burst capability for manoeuvres.



Figure 21: 6S, 45C, 2800mAh, LiPo Battery

The propellers chosen were 6030 tri-blade propellers (6 inch diameter, 3 inch pitch), as shown in *Figure 22*. Tri-blade was chosen over bi-blade due to greater thrust at the same RPM, allowing a lower RPM and reducing current draw.



Figure 22: 6030 Tri-Blade Propeller

The chosen servo motors were MG-90S servo motors, shown in *Figure 23*. While the rotation mechanism was designed with SG-90 motors, the MG-90S has an identical shape and size. The MG-90S offers 2.2kg/cm of torque as compared to the SG-90's 1.8kg/cm, making it stronger without having to alter the design.



Figure 23: MG-90S Servo Motor

The chosen radio controller was a FlySky FS-i6X, shown in *Figure 24*. This was due to its native integration with iBus, which would make movement control much more efficient and work through a single signal wire. It also offers reliable AFHDS 2A communication, and can expand from 6 channels to 10 channels if needed.



Figure 24: FlySky FS-i6X

The chosen receiver was a FS-iA6B module, shown in *Figure 25*. Since only 6 channels were needed, this was the default receiver from the same brand as the radio controller.



Figure 25: FS-iA6B

Component	Rated Current	Expected Current (or measured)	Safety Margin
Battery (6S, 45C)	126 A continuous	Peak 81 A (measured)	+56%
PDB, total	140 A continuous	Peak 81 A	+73%
PDB, per ESC pad	60 A	~20 A per motor at measured peak	+200%
ESCs	50 A	~20 A per motor at measured peak	+150%
XT60 connector	30 A continuous, 60 A burst	23 A to 81 A (measured)	+30% to –26%
FC Servo BEC	8 A continuous	2.8 to 4 A	+100% or more

Table 2: Electrical Power Rating-Margin Table

The 6S 2800 mAh pack stores approximately 62.2 Wh (22.2 V × 2.8 Ah). Using 80% of capacity to avoid over-discharge (2.24 Ah) and the measured hover current of 23 A, the estimated hover endurance is approximately 5.8 minutes.

Link	Protocol	Reasoning
Receiver → FC	iBus (serial)	All 6 channels on a single wire; digital, so less noise than separate analog signals
FC → ESCs	PWM	Simple setup and calibration in Mission Planner; default because there's no DShot
FC → Servo Motors	PWM (50Hz)	Standard control signal for the MG-90S
PDB → FC	Analog	Sensor outputs a voltage proportional to current, which the FC's ADC reads for battery monitoring

Table 3: Communication Protocols Used

Endpoints	Connection
Motor 1 ←→ ESC 1 Motor 2 ←→ ESC 2 Motor 3 ←→ ESC 3 Motor 4 ←→ ESC 4	3-phase wires for each motor soldered to the 3 wires of the corresponding ESC
ESC 1 ←→ PDB ESC 2 ←→ PDB ESC 3 ←→ PDB ESC 4 ←→ PDB	Each positive/negative ESC wire soldered to a corresponding positive/negative PDB terminal
PDB ←→ Battery	XT60 male connector soldered to PDB's positive/negative input pads, then connected to Battery's in-built female XT60 connector
ESC 1 ←→ FC ESC 2 ←→ FC ESC 3 ←→ FC ESC 4 ←→ FC	Each ESC's signal wire connected to an FC signal pin (S1, S2, S3, S4), and ground wire connected to ground rail
Servo 1 ←→ FC Servo 2 ←→ FC Servo 3 ←→ FC Servo 4 ←→ FC	Each servo's signal wire connected to an FC signal pin (S5, S6, S7, S8), power wire connected to Vx, and ground wire connected to ground rail
FC ←→ PDB	VBat/G pins from PDB connected to positive/negative input power pads on FC
Receiver ←→ FC	Signal wire connected to the RX6 pin, power wire connected to the 4v5 pin, and ground wire connected to a G pin

Table 4: Electrical Connections in the Circuit

Using the planned electrical connections, a circuit schematic was created, shown in *Figure 26*.

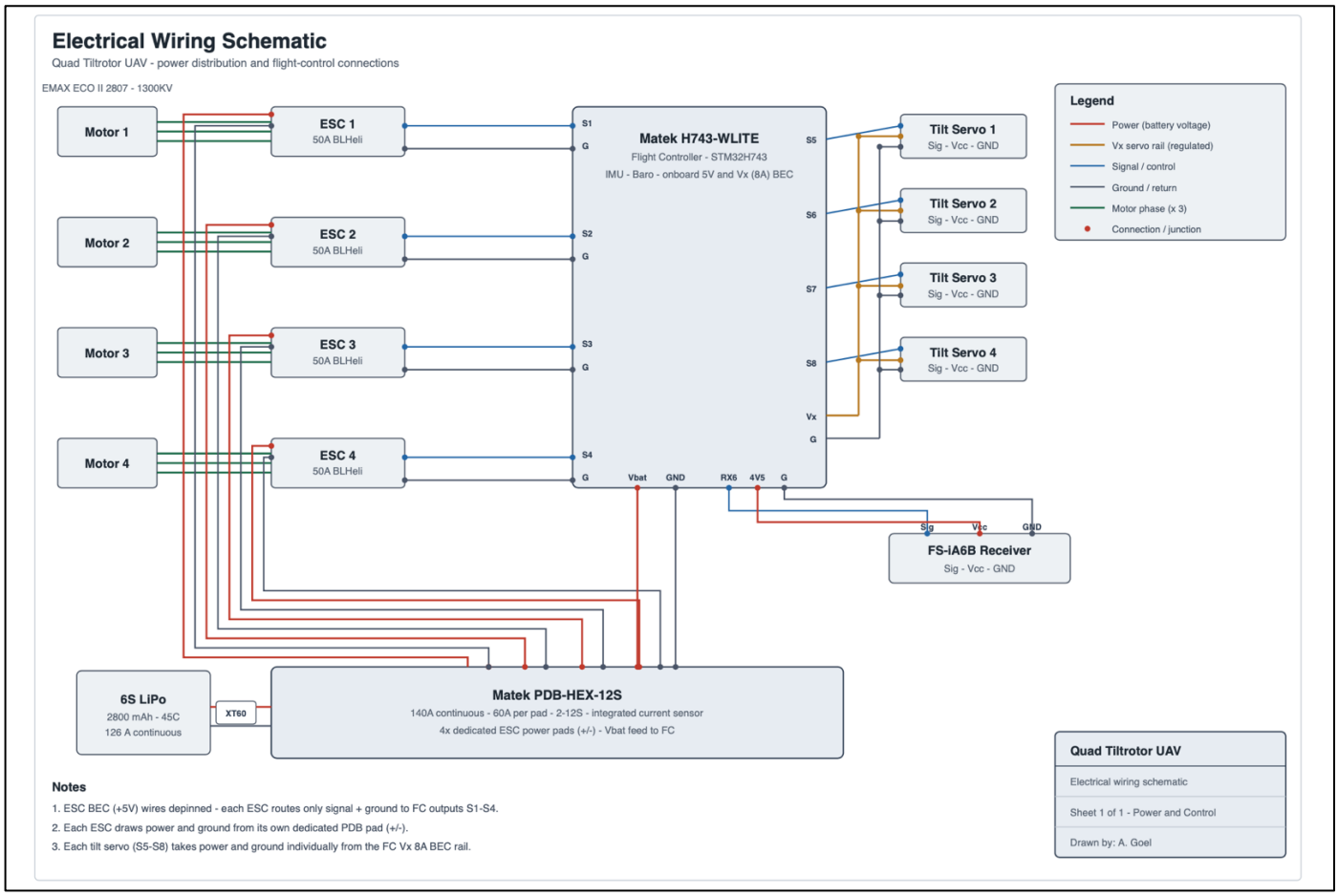


Figure 26: Electrical Wiring Schematic for the Circuit

Hazard	Mitigation Strategy
Propellers (Extremely High RPM)	Bench testing without propellers; wear safety goggles when propellers are on
Battery (Thermal Runaway Explosion)	Use balance charger; keep away from open flames; never leave charging unattended
Signal Loss	Configure ArduPilot's failsafe mechanism to QLAND
Structural Failure	Use a high-infill setting on 3D-printer; conduct low-range tests first before longer flights

Table 5: Risk Assessment

IV. CHASSIS DESIGN

With the electronics and circuitry sorted, the rest of the chassis was designed. The components which needed to be accommodated for in the chassis were the main motors, the flight controller, the PDB, the battery, and the receiver.

Starting with the flight controller, it needed to be secured in a way that the upper surface was exposed for ESC and servo connections. There also needed to be a gap for the two wires that powered the flight controller from the PDB. This is shown in *Figure 27* and *Figure 28*.

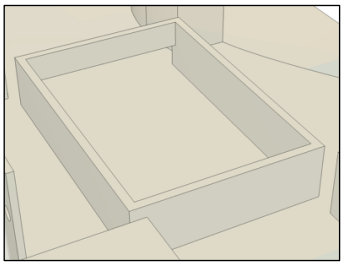


Figure 27: CAD Design of Casing to Hold Flight Controller

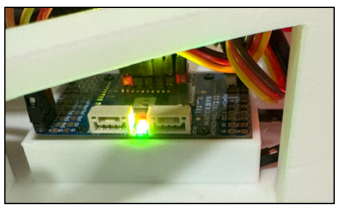


Figure 28: Flight Controller Secured in its Casing

The main propulsion motors needed to be screwed to the arms, thus measurements were taken then holes were engraved. Furthermore, a hole was created in the main body for the wires to go through. This is shown in *Figure 29* and *Figure 30*.

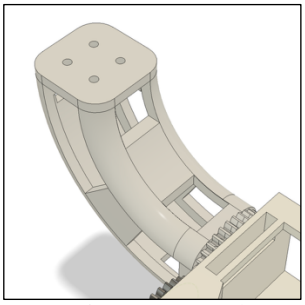


Figure 29: CAD Design of Drone Arm with Screw Holes for Motor



Figure 30: Motor with Propeller Secured onto Drone Arm with Wires through Guidance Hole

The PDB needed to be screwed to the main body, thus measurements were taken, then holes were engraved. This is shown in *Figure 31* and *Figure 32*.

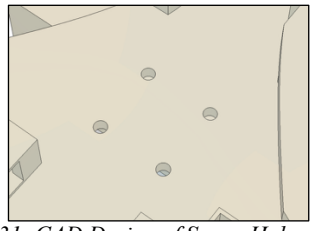


Figure 31: CAD Design of Screw Holes for PDB

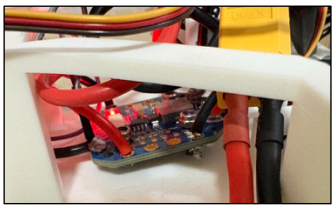


Figure 32: PDB Secured to Main Drone Body

The battery needed a separate compartment to be stored. This was measured then kept below the main drone body, as shown in *Figure 33* and *Figure 34* and was also lined with double-sided tape to secure the battery but allow it to be pulled out for charging.

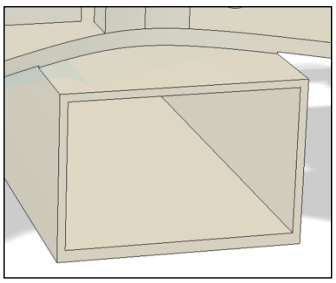


Figure 33: CAD Design of Battery Compartment

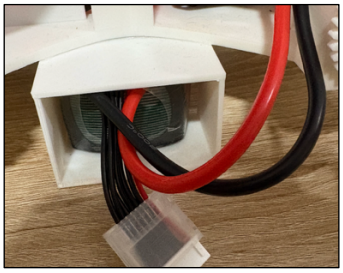


Figure 34: Battery Compartment in Use

The receiver was secured to the top of the chassis using double-sided tape as well, allowing it to be easily removed if required. Furthermore, its antennae were also taped down to the drone frame to prevent clashing with the motors.

After the component specific designs were implemented, the final chassis design was ready, shown in *Figure 35*.

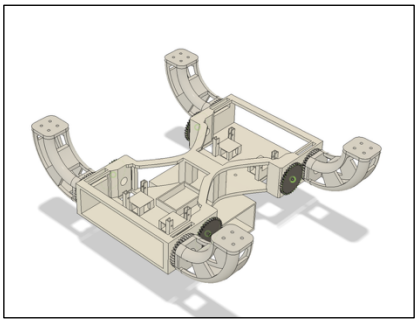


Figure 35: CAD Design Ready for Print (Without Components)

To complete the CAD render, propulsion and servo motors were added, along with the propellers, servo horns, and servo rotation shafts, shown in *Figure 36*.

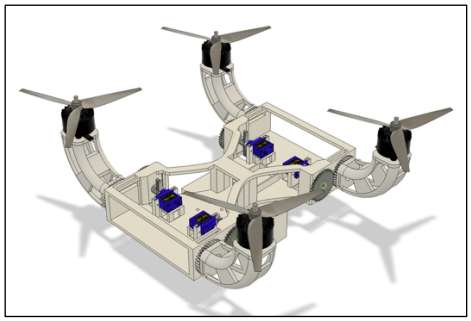


Figure 36: Completed CAD Design with some Components

V. FABRICATION & ASSEMBLY

The different sub-parts of the CAD design were 3D-printed using white PLA plastic. Before assembly, the threaded heat inserts were melted into the rotary shaft pieces. After that, bearings and screws were used for assembly as planned.

Choosing standard PLA filament allowed for rapid, cost-effective prototyping of all the structural components. The trade-off of this material choice compared to ABS, PETG-CF, or PA-CF was PLA's rigidity and lower fatigue resistance under high motor vibration, which made the arm mounts vulnerable to vibrations and possibly even stress fractures.

After the design was assembled, the circuit was assembled in the drone chassis itself. Motor-to-ESC, ESC-to-PDB, and XT60-to-PDB connections were directly soldered together, while all other connections involved the use of header pins, allowing them to be removed if needed. Exposed solder connections were covered by electrical tape to prevent the circuit from shorting.

After the circuit was fully joined together, all the components were secured to the chassis as planned. The propellers were secured to the main motors with locking nuts tightened with an adjustable wrench.

After everything was secured and connected as planned, the drone was fully complete, as shown in *Figure 37*.

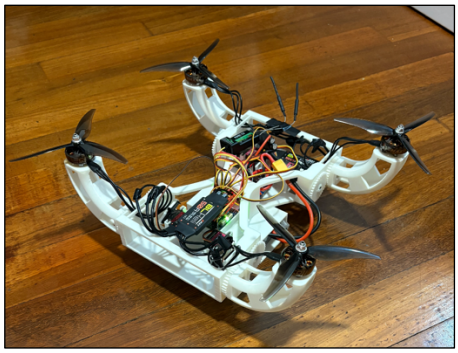


Figure 37: Fully Assembled Drone Ready for Use

VI. CONTROL SETUP

The drone's settings needed to be configured, especially the tiltrotor capability, which was done through the Mission Planner app that natively supports ArduPilot [2]. Within ArduPilot, ArduPlane firmware was chosen and flashed to the flight controller over ArduCopter firmware, due to its support for tilt capabilities that ArduCopter doesn't have.

ArduPlane has multiple "Q" settings that can be configured to support tilt [1]. The feature is intended for transitioning between purely vertical and purely horizontal flight on fixed-wing planes. However, if all flight modes are set to "Q" configurations, the drone will use tilt for vectored motion instead of ever transitioning to a purely forwards setup, perfectly satisfying the desired functionality.

Table 6 shows the different flight modes that were assigned to the drone, each via a different flight channel through the radio controller.

Flight Mode	Autopilot Control	Pilot Control
QSTABILISE	Attitude	Altitude, position, yaw
QHOVER	Attitude, altitude	Position, yaw
QLAND	Descent and touchdown	Negligible (slight nudging)

Table 6: Different Flight Modes Used

The failsafe setting was set to QLAND.

Beyond that, *Table 7* shows the other key settings that were configured to the drone, along with the exact numerical value for the specific functionality.

Setting	Value	Purpose/Meaning
Q_ENABLE	1	Activates code for QuadPlane (VTOL)
Q_FRAME_CLASS	1	Defines the airframe as a Quad
Q_FRAME_TYPE	1	Defines X-shaped layout
Q_TILT_ENABLE	1	Enables tiltrotor servo control
Q_TILT_MASK	15	Bitmasks all motors as tilting
Q_TILT_TYPE	0	Ensures rotors continuously tilt together
Q_TILT_RATE_UP	40	Max tilt slew rate from vertical to forward
Q_TILT_RATE_DN	40	Max tilt slew rate from forward to vertical
SERVO1-4_FUNCTION	33-36	Assigns S1-S4 pins as main propulsion motors
SERVO5-8_FUNCTION	41	Assigns S5-S8 as tilt servo motors

Table 7: Key Settings Configured in Mission Planner

The first four settings in *Table 7* are basic settings that enable tilt functionality and define the drone's layout, and the fifth setting assigns tilt logic to all four motors.

The sixth setting was deliberately set to all rotors tilting together. While allowing each arm to rotate differently was possible, that would cause the tilting mechanism to control yaw as well, which could be more unstable than standard yaw that uses motor speed differentials. This decision directly influenced the outcome by preventing complex vector-assisted yaw coupling, allowing standard differential motor speeds to handle yaw and making PID tuning far more manageable.

The seventh and eighth settings were set to 40 degrees per second for rotation, as that seemed to strike a good balance between quick response and mechanism stability. Selecting a moderate tilt slew rate of 40°/second prevented sudden centre-of-gravity shifts and reduced shock loading on the 3D-printed spur gears during transitions, providing smoother mechanical rotation and lowering the risk of an accident.

The last two settings in the table assigned all propulsion motors to their own signal pin, and then assigned each of the servo motors on different pins to a common role to ensure they rotated in unison.

After all the settings were configured, basic calibrations were done, including the accelerometer, radio controller, and ESCs (through PWM protocol). Finally, the drone was ready to fly.

VII. RESULTS

After initial testing, the drone flew successfully. Hover was nearly flawless, and during forward motion, the main body stayed mostly stable, though servo tilt did lead to slight shaking. Minor PID adjustments were made for each of the three axes to improve flight stability. With a proper PID-tuning rig, this would be more accurate.

Against the success criteria defined in the Aim and Objectives section, all criteria were reasonably met, with particular success for criteria 2 and 3. For criterion 5, the flight log showed the main body's pitch angle staying within approximately 6.5º of level during forward flight.

VIII. LEARNINGS AND FUTURE IMPROVEMENTS

Ultimately, this project was successful, as the stated aim and objectives were met and a fully functional quad-tilt-rotor drone was built and flown. Based on the successful test flights described in Section VII, with a bit more PID tuning this concept could genuinely improve stability, which could have an impact in areas that require long flights and require maximum efficiency. To develop the project in the future, the first thing I need to do is account for the vibrations experienced during arm rotation, which contributed to both the minor gear backlash noted in Section II and the slight body shaking observed during test flights in Section VI. I can address this by using PA-CF or PETG-CF instead of PLA for the arm mounts, and by using a smoother, metal-geared servo motor in place of the MG-90S used here. Another future change could be the use of an XT90 connector, as this would keep it within the safety margin during long bursts. Thirdly, by incorporating an external compass module into the circuit, I could add flight modes such as QLOITER or QRTL which could add extra functionality and make the failsafe more effective.

These changes could reduce mechanical vibrations, simplify PID tuning, and make the drone more effective for future data collection on the efficiency capabilities of tilt-rotor drones.

IX. REFERENCES

[1] ArduPilot Dev Team, "Tilt Rotor Planes," *ArduPilot Plane Documentation*. [Online]. Available: https://ardupilot.org/plane/docs/guide-tilt-rotor.html

[2] ArduPilot Dev Team, "QuadPlanes," *ArduPilot Plane Documentation*. [Online]. Available: https://ardupilot.org/plane/docs/quadplane-support.html

[3] Mateksys, "H743-WLite Flight Controller — Quick Start Guide." [Online]. Available: https://www.mateksys.com/downloads/Manual/H743-WLITE_Manual.pdf

[4] Mateksys, "PDB-HEX, 12S compatible." [Online]. Available: https://www.mateksys.com/?portfolio=pdb-hex

[5] EMAX, "ECO II 2807 Brushless Motor." [Online]. Available: https://shop.emax-usa.com/products/eco-ii-2807-brushless-motor-1300kv-1500kv-1700kv

[6] EMAX, "BLHeli Series 50A UBEC ESC." [Online]. Available: https://emaxmodel.com/products/blheli-series-50a-ubec

[7] A. Misra, R. Behera, and S. Nayak, "A Review on Vertical Take-Off and Landing (VTOL) Tilt-Rotor and Tilt Wing Unmanned Aerial Vehicles (UAVs)," *Journal of Engineering*, vol. 2022, 2022. [Online]. Available: https://onlinelibrary.wiley.com/doi/10.1155/2022/1803638